

# DISTRIBUTED VELOCITY-MATCHED 1.55 $\mu$ m InP TRAVELLING-WAVE PHOTODETECTOR FOR GENERATION OF HIGH MILLIMETERWAVE SIGNAL POWER

M. Alles, U. Auer\*, F.-J. Tegude\*, and D. Jäger

FG Optoelektronik, \*FG Halbleitertechnik/Halbleitertechnologie,  
Gerhard-Mercator-Universität Duisburg, D-47048 Duisburg, Germany

## ABSTRACT

A novel travelling-wave (TW) photodetector for operation at 1.3/1.55  $\mu$ m is fabricated using InP MMIC technology. The results of an optoelectronic simulation are discussed, where photoconductivity effects and phase-matching due to slow-wave effects are included. Theoretical and experimental results of power conversion efficiencies are finally presented.

## INTRODUCTION

Recently, rapid progress has been made in the development of high-speed photodetectors, which are key elements for future millimeterwave photonic communication systems. Especially travelling-wave (TW) photodetectors are regarded to play an important role for the detection of electrical signals at high frequencies not limited by usual RC time constants.

Giboney et al. [1,2] described a 1  $\mu$ m  $\times$  7  $\mu$ m travelling-wave photodetector for an optical wavelength of 830 nm using the AGaAs/GaAs material system. The fabricated photodetector with a bandwidth of 190 GHz exhibited an efficiency of up to 0.45 A/W by using a phase matched structure. Effects arising from high optical input powers have also been discussed. Hietala et al. [3] also discussed a phase-matched travelling-wave photodetector for the detection of millimeterwave signals. They presented a distributed pin-photodetector for an operation at an optical wavelength of 1  $\mu$ m and studied the limitations of the generated

millimeterwave power. The fabricated devices on the basis of AlGaAs/GaAs showed a bandwidth of ca. 5 GHz. Moreover, Lin et al. [4] used a velocity-matched distributed photodetector on the basis of an array of small MSM-diodes connected to each other via electrical and optical waveguides. The operation wavelength of this device was 860 nm and the bandwidth of the fabricated device was about 50 GHz. Jasmin et al. [5] presented also a distributed pin-photodetector but with nonuniform absorption. This device showed reduced saturation effects at high optical input powers and a linear response up to a photocurrent of 8 mA. The fabricated photodetector was not phase-matched, and measurements at a wavelength of 1.55  $\mu$ m revealed a bandwidth of 20 GHz.

On the other hand, optoelectronic techniques for the generation of high power millimeterwaves were first proposed by Soohoo et al. in 1981 [6]. In this approach, a heterodyne signal generates a millimeterwave in a distributed Schottky-photodiode. Such a device is therefore a key element in analogue optical links where millimeterwave signals are optically transmitted using fibres. It should, however, be mentioned that in contrast to the usual application of a photodetector such a component should exhibit a high power conversion efficiency, preferably with gain.

As can be seen, up to now most of the published results address the high-speed behavior of the travelling-wave photodetector and the quantum efficiency, but less work has been dedicated to the power conversion

efficiency and the electrical output power at millimeterwave frequencies and optical wavelengths of  $1.3\text{ }\mu\text{m}$  or  $1.55\text{ }\mu\text{m}$ .

In this paper we present a novel travelling-wave photodetector which has especially been designed for a high power conversion efficiency at millimeterwave frequencies and optical wavelengths of  $1.3\text{ }\mu\text{m}$  and  $1.55\text{ }\mu\text{m}$ . The device is fabricated using an optoelectronic CAD tool developed for microwave optical interaction devices and using standard InP MMIC technology.

## DESIGN OF THE TW-PHOTODETECTOR

The structure of the fabricated travelling-wave photodetector is depicted in Fig. 1. The device is MBE-grown on semi-insulating InP-substrate. First, the optical waveguide consisting of InGaAlAs is grown, followed by the optical absorbing InGaAs layer. The epitaxy is completed with an InAlAs cladding and an InAlAs/AlAs Schottky barrier enhancement layer. Electrical waveguiding is achieved by using a coplanar transmission line where the center conductor forms a Schottky contact to the semiconductor leading to slow-wave effects [7]. Additionally, the Schottky contact provides a depletion layer, which is used to separate the photogenerated electron-hole-pairs in the absorbing layer. The outer conductors form

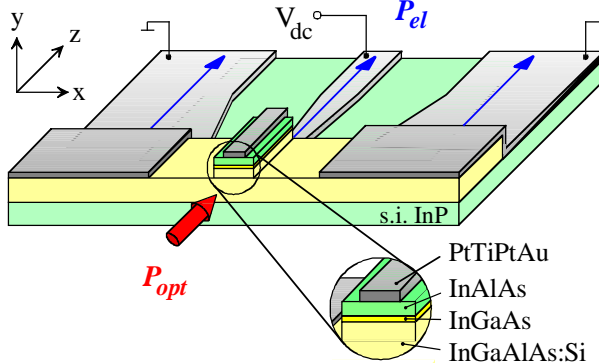


**Fig. 1:** Schematic view of the travelling-wave photodetector.  $P_{\text{opt}}$  and  $P_{\text{el}}$  are the input optical and the output electrical power, respectively. The taper facilitates hybrid coupling with MMICs

ohmic contacts to the n-doped quarternary layer. The electrical transmission line is further connected to a taper for hybrid integration using flipchip- or wire bonding [8].

The structure of the travelling-wave photodetector has been designed concerning optical and electrical wave propagation effects and the optoelectronic interaction in the region of the overlapping field. In the present case, the optical simulation of the travelling-wave photodetector is done using a beam propagation method to determine the optical intensity distribution. This allows the calculation of the distributed photocurrent as a wave function in space and time. The optoelectronic interaction and the electrical propagation are finally determined from the distributed equivalent circuit model depicted in Fig. 2. Here  $W_m'$  is the impedance of the metallic layers,  $L'$  the inductance of the transmission line, and  $R'$  the longitudinal resistance of the semiconductor.  $C'$  and  $G'$  are the capacitance and the conductance of the depletion layer, respectively. The distributed current source  $I_{\text{ph}}$  parallel to  $C'$  and  $G'$  describes the impressed photocurrent in the absorbing layer. The conductance  $G_B'$  results from the conductivity of the bulk material. Finally, the capacitance  $C_L'$  describes the

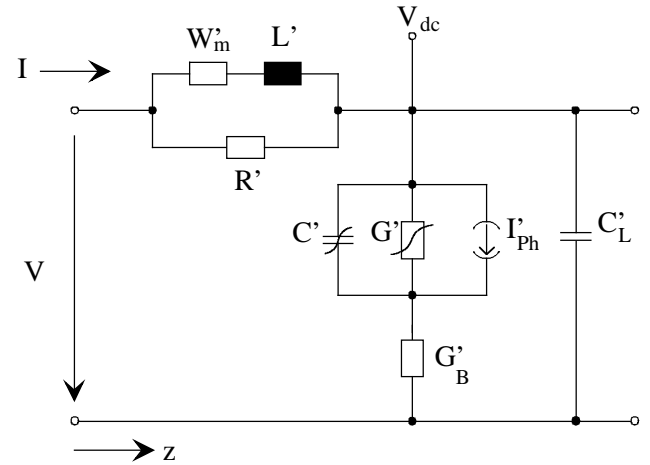


**Fig. 2:** Equivalent circuit model for the travelling-wave photodetector. All elements are per unit length, cf. [7]

electrical field of the coplanar waveguide in air. The different equivalent circuit elements have been measured up to frequencies of 60 GHz using network analysis. The results are shown in Tab. 1. From the equivalent circuit and the parameters of the experimental line, the group velocity is determined and matched to the velocity of the optical envelope to ensure a maximum conversion efficiency. This is achieved in the present case by using the slow-wave effects of the coplanar transmission line leading to a clear distributed interaction.

$L'$	0.466 nH/mm	$G'$	67 fS/mm
$\text{Re}\{W_m\}$	$6.58 \Omega/\text{mm}$	$G'_b$	$874 \text{ S/mm}$
$R'$	$707 \Omega/\text{mm}$	$C'_L$	$0.16 \text{ pF/mm}$
$C'$	$1.39 \text{ pF/mm}$		

**Tab. 1:** Measured values for the equivalent circuit in Fig. 2

## THEORETICAL AND EXPERIMENTAL RESULTS

The equivalent circuit can now be used to calculate the electrical output power. For the device under study, a millimeterwave power of up to -18.3 dBm is obtained for an optical input power of 0 dBm per carrier at a frequency of 60 GHz and a wavelength of  $1.55 \mu\text{m}$ . We have further studied photoconductive effects in our device which are represented by the photoconductor  $G'$  in the equivalent circuit of Fig. 2. Now  $G'$  is a function of space and time corresponding to  $I'_{\text{ph}}$  and an applied bias voltage  $V_{\text{dc}}$  can be used to generate a millimeterwave along the transmission line, where the output power depends quadratically on the bias voltage [9]. Fig. 3 shows the result of a simulation, i.e. millimeterwave output amplitude vs. bias voltage.

The fabricated travelling-wave photodetectors have been measured in the frequency domain using a heterodyne setup at  $1.55 \mu\text{m}$  consisting of two  $1.55 \mu\text{m}$  tunable erbium fiber lasers, an on-wafer probe and a spectrum

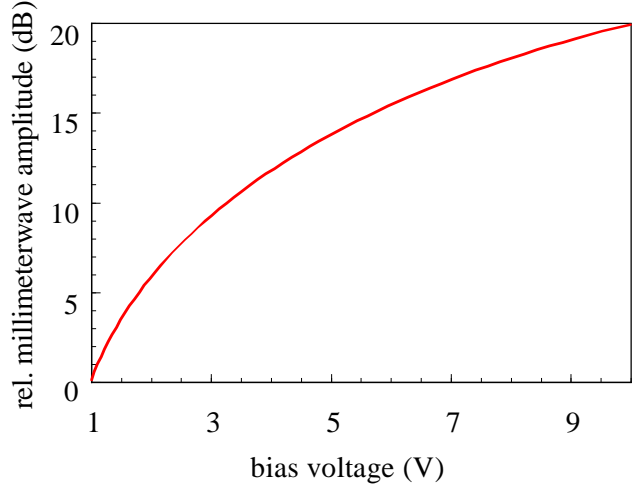


**Fig. 3:** Simulated response of the travelling-wave photoconductor vs. applied bias voltage.

analyzer or a power meter with a characteristic impedance of  $50 \Omega$  for measurements up to 60 GHz. As a first result, the generated millimeterwave output power as a function of the bias voltage at 40 GHz is shown in Fig. 4. As can be seen the electrical output power saturates at a reverse bias voltage of about 11 V. Further the frequency response of a travelling-wave photodetector is depicted in Fig. 5. It is obvious that the electrical signal shows only a slight

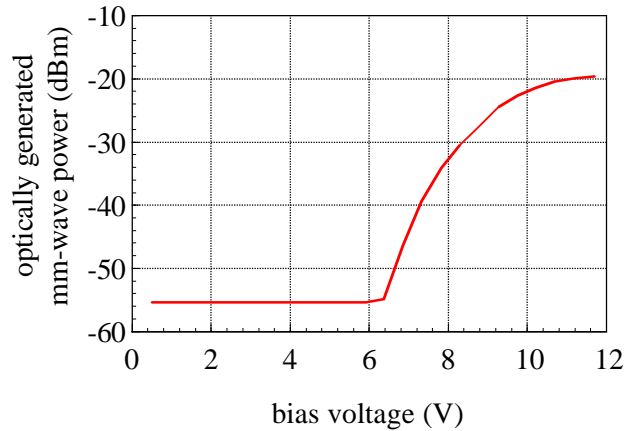


**Fig. 4:** Optically generated electrical millimeter-wave power, measured at 40 GHz. The length of the active region of the travelling-wave photodetector is about  $350 \mu\text{m}$ . The optical input power of the heterodyne signal is 0 dBm per optical carrier. Optical wavelength is  $1.3 \mu\text{m}$ .

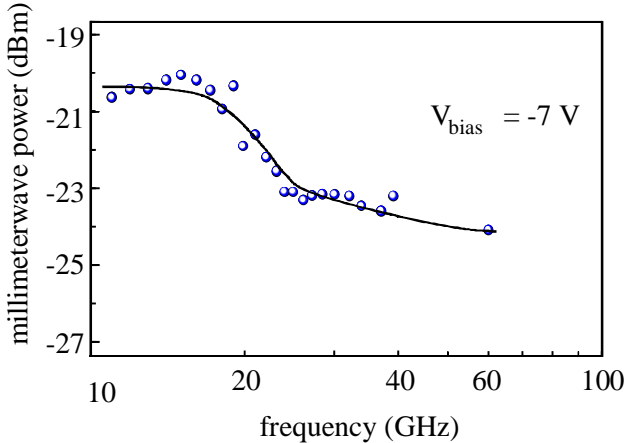


**Fig. 5:** Measured frequency response of the travelling-wave photodetector, optical wavelength  $1.3 \mu\text{m}$ .

decay with frequency, indicating that the fabricated devices show no RC-time limitation. Moreover, the measurements reveal that an efficiency of approximately  $0.3 \text{ A/W}$  can be achieved at  $60 \text{ GHz}$ , where electrical output powers of more than  $-15 \text{ dBm}$  have been measured up to now.

## CONCLUSIONS

In this paper it has been shown both theoretically and experimentally that TW photodetectors can successfully be used to convert optical into millimeterwave power with high efficiency. A comparison with data from the literature finally shows that TW photodetectors seem to have advantages with respect to waveguide photodetectors and vertically illuminated components.

## ACKNOWLEDGEMENT

The authors would like to thank Alcatel SEL AG, Stuttgart, and the Bundesministerium für Bildung, Wissenschaft, Forschung und Technologie (BMBF), Germany for financial support under project number 01BP460/0. Furthermore, the authors wish to thank Dr. I.

Jäger for simulations of the travelling-wave photoconductor.

## REFERENCES

- [1] K.S. Giboney, M.J.W. Rodwell, J.E. Bowers, "Traveling-wave photodetector theory", *IEEE Trans. Microwave Theory and Techn.*, Vol. 45, pp. 1310-1319, 1997
- [2] K.S. Giboney, M.J.W. Rodwell, J.E. Bowers, "Traveling-wave photodetector design and measurement", *IEEE J. of Selected Topics in Quantum Electron.*, Vol. 22, No. 3, pp. 622-629, 1996
- [3] V.M. Hietala, G.A. Vawter, T.M. Brennan, B.E. Hammons, "Traveling-wave photodetectors for high-power, large bandwidth applications", *IEEE Trans. Microwave Theory and Techn.*, Vol. 43, pp. 2291-2298, 1995
- [4] L.Y. Lin, M.C. Wu, T. Itoh, T.A. Vang, R.E. Muller, D.L. Sivco, A.Y. Cho, "High-power high-speed photodetectors-design, analysis, and experimental demonstration", *IEEE Trans. Microwave Theory and Techn.*, Vol. 45, No. 8, pp. 1320-1331, 1997
- [5] S. Jasmin, N. Vodjdani, J.-C. Renaud, A. Enard, "Diluted- and distributed-absorption microwave waveguide photodiodes for high efficiency and high power", *IEEE Trans. Microwave Theory and Techn.*, Vol. 45, pp. 1337-1341, 1997
- [6] J. Soohoo, S.-K. Yao, J.E. Miller, R. Shurtz, II, Y. Taur, R.A. Gudmundsen, "A laser-induced traveling-wave device for generating millimeter waves", *IEEE Trans. Microwave Theory and Techn.*, Vol. 29, No. 11, pp. 1174-1181, 1981
- [7] D. Jäger, "Slow-wave propagation along variable Schottky contact microstrip line", *IEEE Trans. Microwave Theory and Techn.*, Vol. 24, pp. 566-573, 1976
- [8] M. Alles, Th. Braasch, D. Jäger, "High-speed coplanar Schottky travelling-wave photodetectors", *Integrated Photonic Research*, Proc. pp. 380-383, Boston, USA, 1996
- [9] S. Verghese, K.A. McIntosh, E.R. Brown, "Highly tunable fiber-coupled photomixers with coherent Terahertz output power", *IEEE Trans. Microwave Theory and Techn.*, Vol. 45, No. 8, pp. 1301-1309, 1997